Chin. J. Astron. Astrophys. Vol. 7 (2007), No. 5, 669–674
(*http://www.chjaa.org*)

Chinese Journal of
Astronomy and
Astrophysics

Shallow Decay of X-ray Afterglows in Short GRBs: Energy Injection from a Millisecond Magnetar? *

Yu Yu[1] and Yong-Feng Huang[2]

[1] Shanghai Astronomical Observatories, Chinese Academy of Sciences, Shanghai 200030
yuy@mail.ustc.edu.cn
[2] Department of Astronomy, Nanjing University, Nanjing 210093

Received 2007 January 18; accepted 2007 June 7

Abstract With the successful launch of *Swift* satellite, more and more data of early X-ray afterglows from short gamma-ray bursts have been collected. Some interesting features such as unusual afterglow light curves and unexpected X-ray flares are revealed. Especially, in some cases, there is a flat segment in the X-ray afterglow light curve. Here we present a simplified model in which we believe that the flattening part is due to energy injection from the central engine. We assume that this energy injection arises from the magnetic dipole radiation of a millisecond pulsar formed after the merger of two neutron stars. We check this model with the short GRB 060313. Our numerical results suggest that energy injection from a millisecond magnetar could make part of the X-ray afterglow light curve flat.

Key words: gamma rays: bursts — X-rays: individual (GRB 060313) — ISM — stars: neutron

1 INTRODUCTION

Gamma-ray bursts (GRBs) are divided into two classes according to their duration and hardness: long bursts and short bursts. Until the launch of *Swift* Gamma-ray Burst Explorer in Nov. 2004 (Gehrels et al. 2004), afterglow emission was detected only in long GRBs. Thanks to the rapid localization of *Swift*, we have learned more about short GRBs (for a most recent review, see Zhang 2007). In the leading short GRB model, the merger of a compact-object binary, e.g. neutron star-neutron star (Eicher et al. 1989) or neutron star-black hole (Paczyński 1991), was supported by the recent observations.

By the end of 2006, *Swift* has been triggered by more than ten short GRBs (Zhang 2007). Their afterglow light curves show some interesting features. In the X-ray band, a canonical behavior (steep decay–shallower than normal decay–normal decay) is found in GRBs 050509 (Gehrels et al. 2005), 050724 (Berger et al. 2005) and 051221A (Soderberg et al. 2006), but X-ray flares are unexpectedly observed in a good fraction of GRBs, e.g. GRBs 050724 (Berger et al. 2005) and 051210 (La Parola et al. 2006). It seems that X-ray flares and shallower than normal decay segment are mutually exclusive. This puts a restriction on both the models interpreting X-ray flares and those interpreting the shallower than normal segment (Zhang 2007).

GRBs 051221A and 060313 are good examples in which a flat segment can be clearly seen in the middle part of the X-ray afterglow light curve. It has been widely argued that the flattened part is due to post-burst energy injection. Two types of source of this energy were proposed. (i) During a burst, an outflow with varying Lorentz factors is ejected. Materials with lower Lorentz factors will finally catch up with the forward shock when the forward shock decelerates, resulting in a smooth and gradual energy injection into afterglow shock (Rees & Mészéros 1998; Sari & Mészáros 2000). In this model it is usually assumed that

---

* Supported by the National Natural Science Foundation of China.

the mass and energy associated with materials with Lorentz factors greater than given Γ obey a power law function, $M\,(>\Gamma) \propto \Gamma^{s}$ and $E\,(>\Gamma) \propto \Gamma^{1-s}$. In order to cause a shallower decay, the total energy should gradually increase with time, which means $s > 1$. This leads to an upper limit for the increase in the temporal decay index (i.e., $\Delta\alpha$) across the break point (for details of the calculations see Nousek et al. 2006), which may not be consistent with some GRBs. (ii) The energy injection arises from a long lasting central engine (Dai & Lu 1998a,b; Zhang & Mészáros 2001; Dai 2004; Fan & Xu 2006). This scenario is not subject to the maximum $\Delta\alpha$ encountered by the varying Lorentz factor model.

In this paper we focus on the possibility of energy injection from a millisecond pulsar. The millisecond pulsar may have formed after the merger of two neutron stars (Dai et al. 2006). Its magnetic dipole radiation supplies energy into the forward shock, which makes the afterglow light curve flat. We first give some theoretical analysis and then apply the model to GRB 060313.

2 ENERGY INJECTION

2.1 Dynamics

Consider the adiabatic case. Let R be the radial coordinate in the burster frame, γ the Lorentz factor, n the number density of surrounding interstellar medium (ISM), and $m_{\rm p}$ the mass of proton. The total energy of the ejecta ($E_{\rm jet}$) is given by

$$E_{\rm jet} = \frac{\Omega_{\rm jet}}{3} R^3 \gamma^2 n m_{\rm p} c^2, \tag{1}$$

where $\Omega_{\rm jet}$ is the beaming factor. Taking L to represent the isotropic energy injection from a millisecond magnetar, we have

$$\frac{dE_{\rm jet}}{dt} = L \frac{\Omega_{\rm jet}}{4\pi}, \tag{2}$$

where t is observer's time. We assume that the millisecond magnetar has an initial rotation period of P_0, with surface magnetic field strength $B_{\rm s}$, moment of inertia I, radius R_M, and angle between the rotation axis and magnetic dipole moment δ. Then the expression for L can be written as (Dai 2004),

$$L = 4 \times 10^{47} B_{\perp,14}^2 R_{M,6}^6 P_{0,{\rm ms}}^{-4} \left(1 + \frac{t}{T_{M,0}}\right)^{-2} {\rm erg\,s^{-1}}, \tag{3}$$

where $B_{\perp,14} = B_{\rm s} \sin\delta / 10^{14}\,{\rm G}$, $R_{M,6} = R_M/10^6\,{\rm cm}$, $P_{0,{\rm ms}} = P_0/1\,{\rm ms}$, $I_{45} = I/10^{45}\,{\rm g\,cm^2}$ and $T_{M,0} = 5.01 \times 10^4 B_{\perp,14}^{-2} I_{45} R_{M,6}^{-6} P_{0,{\rm ms}}^2 {\rm s}$. Combining Equations (1) – (3), we have:

$$\frac{d\gamma}{dt} = \frac{3L}{8\pi n m_{\rm p} c^2 R^3 \gamma} - \frac{3\gamma}{2R}\frac{dR}{dt} - \frac{\gamma \sin\theta}{2\,(1-\cos\theta)}\frac{d\theta}{dt}, \tag{4}$$

where θ is the half-opening angle of the ejecta.

Let $t_{\rm co}$ be the time measured in the co-moving frame of the jet, and dt_b the time interval of emitting two adjacent photons from the emission region (correspondingly dt is the time interval for the observer to receive the two photons). Denoting the swept-up mass as m, we have the following relations (Huang et al. 1999, 2000a,b):

$$dR = \beta c dt_b, \tag{5}$$

$$dt_b = \gamma dt_{\rm co} = \gamma \left(\gamma + \sqrt{\gamma^2 - 1}\right) dt, \tag{6}$$

$$\frac{dR}{dt} = \beta c \gamma \left(\gamma + \sqrt{\gamma^2 - 1}\right), \tag{7}$$

$$\frac{dm}{dR} = 2\pi R^2 \,(1 - \cos\theta)\, n m_{\rm p}, \tag{8}$$

$$\frac{d\theta}{dt} \equiv \frac{1}{R}\frac{da}{dt} = \frac{c_{\rm s}\left(\gamma + \sqrt{\gamma^2 - 1}\right)}{R}, \tag{9}$$

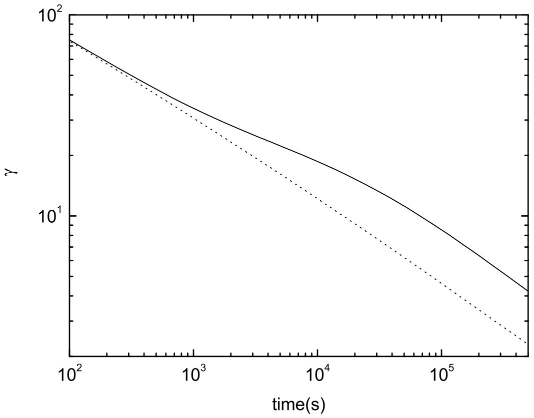

Fig. 1 Evolution of the Lorentz factor. The solid line corresponds to a jet with energy injection, and the dotted line to one without energy injection.

where $\beta = \sqrt{\gamma^2 - 1}/\gamma$, and a is the comoving lateral radius of the ejecta. Let $\hat{\gamma} = (4\gamma + 1)/(3\gamma)$ (Dai et al. 1999), we can give the expression for the comoving sound speed, $c_{\rm s}$: $c_{\rm s}^2 = \hat{\gamma}\,(\hat{\gamma} - 1)\,(\gamma - 1)\,\frac{1}{1+\hat{\gamma}(\gamma-1)}c^2$ (Huang et al. 2000a). From Equation (4), we then have

$$\frac{d\gamma}{dt} = \frac{3L}{8\pi n m_{\rm p} c^2 R^3 \gamma} - \frac{3\beta c \gamma^2 \left(\gamma + \sqrt{\gamma^2 - 1}\right)}{2R} - \frac{\sin\theta c_{\rm s} \gamma \left(\gamma + \sqrt{\gamma^2 - 1}\right)}{2R\,(1 - \cos\theta)}. \tag{10}$$

Equations (7), (8), (9) and (10) give a complete description of the dynamics. We have solved these dynamical evolution equations numerically, by taking the parameters as follows: the initial energy $E_0 = 1 \times 10^{51}$ erg, initial Lorentz factor $\gamma_0 = 300$, $n = 0.01\,{\rm cm}^{-3}$, electron energy fraction $\xi_{\rm e} = 0.1$, magnetic energy fraction $\xi_B = 0.1$, power-law index of electron distribution function $p = 2.5$, $\theta_0 = 0.1$, luminosity distance of the GRB $D_L = 1.0 \times 10^6\,{\rm kpc}$, $B_\perp = 10^{14}\,{\rm G}$, $R_M = 10^6\,{\rm cm}$, $P_0 = 1\,{\rm ms}$ and $I \sim 10^{45}\,{\rm g\,cm}^2$. All of these are typical values under usual conditions.

Figure 1 shows the evolution of the Lorentz factor, with the solid line for the case with energy injection and the dotted line for no energy injection. We see that when $t < 10^3$ s the two lines are very similar to each other. This is because, at this early stage, the injected energy is still relatively small compared to the initial energy of the GRB remnant. The two lines differ markedly in $10^4\,{\rm s} < t < 10^5\,{\rm s}$, indicating that the injected energy is significant at this stage. This is consistent with the spin-down timescale of the millisecond pulsar, $T_{M,0}$. Figure 1 also shows clearly that the Lorentz factor decays slower compared to the case without energy injection, and there is a flat segment to the curve. As the flux density evolves with a similar tendency as the Lorentz factor, we can expect a flat part in the corresponding X-ray light curve.

2.2 Synchrotron Radiation

Let Θ be the angle between the velocity of the emitting material and the line of sight and $\mu = \cos\Theta$, then the observed flux density at frequency ν is (Huang et al. 2000a,b)

$$S_\nu = \frac{1}{A}\left(\frac{dP(\nu)}{d\Omega}\frac{A}{D_L^2}\right) = \frac{1}{\gamma^3\,(1 - \beta\mu)^3}\frac{1}{4\pi D_L^2}P'\left[\gamma\,(1 - \beta\mu)\,\nu\right], \tag{11}$$

where A is the area of the detector. We take the equal arrival time surface effect into account (Waxman 1997; Panaitescu & Mészáros 1998, 1999; Moderski et al. 2000; Huang et al. 2007). Due to the ultra-relativistic motion, the equal arrival time surface is determined by

$$t = \int \frac{1 - \beta\mu}{\beta c} dR \equiv {\rm const.} \tag{12}$$

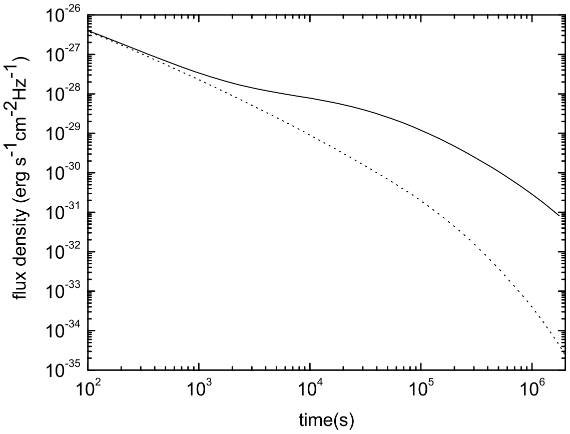

Fig. 2 Evolution of the flux density (at 0.3 keV). The solid line corresponds to a jet with energy injection, the dotted line to one without energy injection.

Using the same parameters above, we obtain the numerical results displayed in Figure 2. Compared to the dotted curve (without energy injection), there is a flat segment in the solid light curve (with energy injection). It supports the idea that energy from a millisecond magnetar injected into the GRB fireball can flatten the X-ray light curve. In the following section we will apply the model to GRB 060313.

3 APPLICATION TO GRB 060313

On 2006 March 13, at 00:12:06.484 UT, GRB 060313 was detected by BAT (Pagani et al. 2006) at RA 66.624, Dec –10.859 (J2000), and its BAT T$_{90}$ is 0.7 second. The X-Ray Telescope (XRT) started observation 79 seconds after the trigger. Copious early X-ray and UV afterglow data are available for this event, which may hopefully provide useful information on the nature of short GRBs (Roming et al. 2006). The X-ray afterglow light curve cannot be described by a single power-law, but shows a three-segment structure. In other words, there is an extra flat segment between $\sim$ 1000 and $\sim$ 10000 seconds. Roming et al. (2006) suggested that this flat segment may be due to a structured jet, but they did not provide a quantified fitting. Here we will use the energy injection model in a re-examination of this event.

Theoretically, due to energy injection there should be two breaks in the afterglow light curve in the X-ray band, one at t_c when the injected energy roughly equals to its initial kinetic energy and one at t_f when the energy injection is turned off (Dai & Lu 1998a; Zhang & Mészáros 2001; Zhang et al. 2006), where t_f is roughly equal to the spin-down time scale $T_{M,0}$ of the magnetar. From the XRT observations of GRB 060313, we measure $t_f \sim 4000\,$s (i.e., $T_{M,0} \sim 4000\,$s), $t_c \sim 2000\,$s. By considering the following relations,

$$\int_0^{t_c} \frac{dE_{\rm jet}}{dt} dt = \int_0^{t_c} L \cdot \Omega_{\rm jet} dt = E_{\rm k}, \tag{13}$$

$$L \sim \frac{E_{\rm k}}{t_c}, \tag{14}$$

we obtain an average injection power $L \sim 3 \times 10^{49}$ erg s^{-1}. So, we take the parameters of the central pulsar as $P_0 = 1\,$ms, $B_s = 10^{14}\,$G, $R_M = 2.0 \times 10^6$ cm and $I = 4.5 \times 10^{45}$ g cm^2, all of which are typical values for a millisecond magnetar.

In the early X-ray observations, we have $f_\nu \propto \nu^{0.53\pm0.10}$ (Roming et al. 2006), so the photon index $p \sim 2.1 \pm 0.2$. Here we take $p = 2.3$. Figure 3 plots our best fitting result for the X-ray afterglow of GRB 060313 using the energy-injection model. In our calculation, the other afterglow parameters are taken as: $E_{\rm k} = 6 \times 10^{52}\,$erg, $\xi_{\rm e} = 0.05, \xi_B = 0.022$, $n = 0.005\,{\rm cm}^{-3}$, $\theta_0 = 0.1$, and the viewing angle $\theta_{\rm obs} = 0$ (i.e. on-beam viewing). These afterglow parameters are generally consistent with the values suggested by Roming et al. (2006). The redshift of GRB 060313 is unfortunately not available, however, to do the calculation we assumed the luminosity distance of the burster to be 2.8×10^6 kpc.

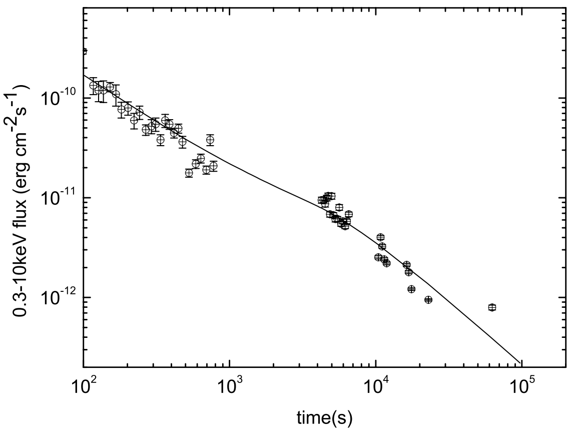

Fig. 3 Fitting result for the 0.3–10 keV X-ray afterglow of GRB 060313. The solid line is the numerical result. The observational data are taken from Roming et al. (2007).

In Figure 3 the solid line represents the numerical result, which fits the observational data points very well, and demonstrates the possibility that the flattened part in the afterglow light curve of this event may be due to energy injection from a central millisecond magnetar.

We have also tried to use our model to fit the UVOT afterglow data of GRB 060313 as observed by Roming et al. (2006). However, our model failed to give a satisfactory result. In fact, the behavior of the optical afterglow is quite different from that of X-ray afterglow: the decay of the optical light curve is much slower, with significant fluctuations superposed. It would be too difficult for a simple external shock model to explain both the X-ray and optical afterglows. This might be a general difficulty in the *Swift* era: in many cases, the optical afterglows were observed to behave quite differently from the X-ray afterglows (Zhang 2007). It is quite possible that the X-ray and optical afterglows may be of different origin in these events.

4 CONCLUSIONS AND DISCUSSION

Swift observations show that early afterglow light curves of many GRBs are unusual in the X-ray band. In this paper we have focused on the shallow decay segment, and explored the energy injection explanation, assuming that the energy source is a millisecond magnetar. We have derived dynamical evolution equations under the adiabatic condition, and carried out numerical calculations to study the process. We applied the model to GRB 060313. The fitting result is good so we believe that this explanation is correct for this event.

Our results are consistent with the leading model for short GRBs, i.e., the merger of two compact stars. After the merger of two neutron stars, which triggers a short GRB, a millisecond pulsar may be left in the center. In the afterglow phase the pulsar's magnetic dipole radiation supplies energy into the GRB remnant, leading to a flat segment in the X-ray afterglow light curve.

In the above consideration, we did not take into account two other factors. First, we assume the energy injection is isotropic, so the energy received by the ejecta is restricted within the opening angle of the ejecta. However, in the real situation the energy may be anisotropic. There probably is some small deviation or fluctuation of the exact injected energy from the value that we used in our calculation. Secondly, we did not consider the influence of the interaction between the injected energy and the originally ejected fireball material (Ma et al. 2003; Mao & Wang 2001a,b). This interaction may lead to additional shocks and emission. Further discussion would be much more complicated.

Acknowledgements We thank the anonymous referee for useful suggestions that lead to an overall improvement of this manuscript. We also would like to thank Z. G. Dai for stimulating discussion, and E. W. Liang for helping accessing some observational data. This research was supported by the National Natural Science Foundation of China (Grants 10625313 and 10221001).

References

Berger E., Price P. A., Cenko S. B. et al., 2005, Nature, 438, 988
Dai Z. G., Lu T., 1998a, A&A, 333, L87
Dai Z. G., Lu T., 1998b, Phys. Rev. Lett., 81, 4301
Dai Z. G., Huang Y. F., Lu T., 1999, ApJ, 520, 634
Dai Z. G., 2004, ApJ, 606, 1000
Dai Z. G., Wang X. Y., Wu X. F. et al., 2006, Science, 311, 1127
Eichler D., Livio M., Piran T. et al., 1989, Nature, 340, 126
Fan Y. Z., Xu D., 2006, MNRAS, 372, L19
Gehrels N., Chincarini G., Giommi P. et al., 2004, ApJ, 611, 1005
Gehrels N., Sarazin C. L., OBrien P. T. et al., 2005, Nature, 437, 851
Huang Y. F., Dai Z. G., Lu T., 1999, MNRAS, 309, 513
Huang Y. F., Gou L. J., Dai Z. G. et al., 2000a, ApJ, 543, 90
Huang Y. F., Dai Z. G., Lu T., 2000b, MNRAS, 316, 943
Huang Y. F., Lu Y., Wong A. Y. L. et al., 2007, Chin. J. Astron. Astrophys. (ChJAA), 7, 397
La Parola V., Mangano V., Fox D. et al., 2006, A&A, 454, 753
Ma H. T., Huang Y. F., Dai Z. G. et al., 2003, Chin. J. Astron. Astrophys. (ChJAA), 3, 225
Mao J. R, Wang J. C., 2001a, Chin. J. Astron. Astrophys. (ChJAA), 1, 349
Mao J. R, Wang J. C., 2001b, Chin. J. Astron. Astrophys. (ChJAA), 1, 433
Moderski R., Sikora M., Bulik T., 2000, ApJ, 529, 151
Nousek J. A., Kouveliotou C., Grupe D. et al., 2006, ApJ, 642, 389
Paczyński B., 1991, Acta Astron., 41, 257
Pagani C., Barthelmy S., Cummings J. et al., 2006, GCN Circ. #4867
Panaitescu A., Mészáros P., 1998, ApJ, 493, L31
Panaitescu A., Mészáros P., 1999, ApJ, 526, 707
Rees M. J., Mészáros P., 1998, ApJ, 496, L1
Roming P. W. A., Berk D. V., Paĺshin V. et al., 2006, ApJ, 651, 985
Sari R., Mészáros P., 2000, ApJ, 535, L33
Soderberg A. M., Berger E., Kasliwal M. et al., 2006, ApJ, 650, 261
Waxman E., 1997, ApJ, 491, L19
Zhang B., Mészáros P., 2001, ApJ, 552, L35
Zhang B., Fan Y. Z., Dyks J. et al., 2006, ApJ, 642, 354
Zhang B., 2007, Chin. J. Astron. Astrophys. (ChJAA), 7, 1